Powder Technology 361 (2020) 968–982

Contents lists available at ScienceDirect

Powder Technology

journal homepage: www.elsevier.com/locate/powtec

Study of the polymer mortar based on dredged sediments and epoxy resin: Effect of the sediments on the behavior of the polymer mortar

Walid Maherzi *, Ilyas Ennahal, Mahfoud Benzerzour, Yannick Mammindy-Pajany, Nor-Edine Abriak

LGCgE-Laboratoire de Génie Civil et géoEnvironnement, IMT Lille-Douai, CERI Matériaux et Procédés, Univ. Lille, EA 4515, 764 BD Lahure, 59500 Douai, France

ARTICLE INFO

Article history:
Received 3 April 2019
Received in revised form 11 October 2019
Accepted 28 October 2019
Available online 18 November 2019

Keywords:
Sediment
Beneficial reuse
Waste management
Polymer concrete
Sustainability

ABSTRACT

Several studies have shown the potential of upgrading sediments in the civil engineering field. However, the complexity of sediments represents a scientific challenge in terms of their management. This study presents the river sediments recovery in a thermosetting matrix. The characterization results epoxy mortars show the feasibility of incorporating dredged sediments up to 50% substitution rate of natural sand. Moreover, according to the physic, mechanical, thermal and chemical evaluations of the thermosetting matrices, it appears that the performances depend on the factors of the rate of resin and the rate of sediments used. Indeed, the difference between the performances of resin mortars containing sediments and mortars without sediments is reduced by a resin content equal to 18%. In comparison with cementitious matrix mortars, the performances of polymeric mortars are well above. Finally, the SEM observations of different formulations made it possible to explain the results observed at the macroscopic scale.

1. Introduction

In France the river sediments extract represents 6 million m^3 per year [1]. This accumulation gradually reduces the depth of rivers and becomes a constraint for river transport. The river network of Nord-Pas-de-Calais suffers from significant sedimentation, due to the low flows and slopes that characterize its hydrographic network. This phenomenon is fueled by significant inputs suspended matter from urban storm water runoff, erosion of agricultural soils, industrial activities and sanitation networks. Fluvial dredging sediments is mainly composed by fine particles and have a specific physical and chemical characteristics compared with natural aggregates like contaminant: heavy metals (Hg, As, Cr, Tl, Pb, etc.) and organic pollutant (PCB, PAH, etc.) [2,3]. These characteristics imposes a risk of transfer of these to the ecosystem, the organic matter which affects the physical and mechanical properties [4] and by the fact that it [5]. For this Fluvial sediments are considered as waste in accordance with national legislation.

A number of research studies have been carried out in order to reuse sediment as secondary raw materials, like as in sub base materials for road construction [6–8], in cement matrices [9–11], in lightweight aggregates formulation [12,13]. However, they have shown that the use of sediments in cementitious matrices influences the characteristics of fresh concrete (rheology, setting time) [2,14,15] and hardened concrete (strength and durability) [16,17]. Furthermore, recently research [43] was demonstrate the feasibility of used marine and fluvial sediments to make polyester matrix mortars.

The polymer mortar is a composite material comprises a polymeric binder and a hardener and natural mineral aggregates as filler in polymeric materials, such as River Sand [28], standardized siliceous sand [33], crushed basalt [34]. The polymer mortar was developed for the first time in the 50's [18], then became well known in the 70's [19]. Today it is shown that polymer matrix materials have the following advantages: high strength properties [22], fast curing time [23], good chemical resistance [24,25] and corrosion ease of manufacture, and it has a long service life and low permeability. Polymer mortars have been used in several civil engineering applications, mainly used for flooring and repairing cracks in damaged concrete structures, pavements, sewage pipes, hazardous waste containers, several prefabricated products such as acid tanks [20,21]. The performance of polymeric mortars depends on several factors, such as resin content [26,27], the quantity and size of the aggregates [28,29], the nature and the shape of the aggregates [30,69], the bonding between the particle and matrix [31]. Several studies have demonstrated the feasibility of using have used waste such as recycled glass [35], foundry sand [32], fly ash [21,36,37], red mud [38], waste polyethylene terephthalate (PET) [39,40], marble powder waste [41], wood flour [42] and rubber particles [69]. Also, Wang et al. [69] have demonstrated that the added rubber particles can improve the mechanical performance of the epoxy concrete materials, especially on compressive strength and splitting tensile strength.

Our research study carried out the feasibility of reusing sediments as aggregates in a thermosetting polymer matrix. The mechanical strengths of a polymer mortar mainly depend on the intragranular

* Corresponding author.
E-mail address: walid.maherzi@imt-lille-douai.fr (W. Maherzi).

https://doi.org/10.1016/j.powtec.2019.10.104
0032-5910/

Table 1
Characteristics of the used epoxy resin.

Proportions of the mixture	Mix ratio resin to hardener ≥ 2:1
Density	1.1 g / cm^3
Hardness Shore D	70–75
Hardness of the core	70–75 N / mm^2 at 14 days
Heat resistance	+40 °C to +45 °C
Operating temperature	+10 °C to +30 °C
Viscosity	1000–1200 mPa.s

porosity. The formulations of resin mortar were optimized using the Packing Density Model. The purpose of this model is to optimize the granular skeleton to reduce intragranular porosity. Once the granular skeleton was optimized, the resin was added to bind the particles and at the same time to fill the residual intragranular porosity. It is noted that the epoxy resin does not exhibit any significant dimensional change in hardening. Therefore, this optimization method makes it possible to have a better mixture in the hardened state.

2. Materials and characterization

2.1. Resin

The binder used is composed by a solvent-free and transparent epoxy-based castable resin. The hardener was selected with a reaction rate of between 40 min and 50 min. The epoxy resin can be mixed with different fillers and will allow, according to the proportion of resin, to obtain mortars. Table 1 presents the characteristics of the epoxy resin.

2.2. Characterization of aggregates

The sediment used in this study was provided by the waterways authority of France (Voie Navigable de France). It was dredged from the Neufossé channel during the maintenance work done in 2017 (framed area in red on the Fig. 1). The sand used is standardized sand (ISO 679 standardized sand) is natural siliceous sand, especially in the finest fractions. It's clean the grains are of generally isometric and rounded shape. The sediment and sand density was measured using a Micrometrics Accupycs 1330 helium pycnometer model. This test was performed in accordance with standard NF EN 1097–7: (2008). The specific surface area of sediment was also measured in accordance with standard NF EN ISO 18757: (2003), using a Micromeritics Autopore IV 9505 instrument. The evaluation of organic matter content was carried out by the loss on ignition test according to the standard XP P94–0447: (1998) which consist on the calcination at 450 °C for 3 h. The loss of mass is measured and related to the initial dry mass. The methylene blue absorption test (VBS) for the evaluation of the sediment was also carried out in accordance with standard NF P 94–068: (1998). Table 2 presents the physical characterization of the sediments. Determination of the particle size is performed with an LS 13320 laser apparatus. The particle size distribution of the aggregates is shown in the figure (Fig. 2).

The mineralogical characterization of sediment and sand is carried out essentially by X-ray diffraction analysis (XRD). The analysis is carried out using a device of the Siemens D5000 type and consists of a measurement of the intensity and the diffraction angles pertaining to the internal atomic structuring. This is completed by an X-ray fluorescence (FX) analysis to determine quantitatively the chemical elements involved. The results indicate that the sediment composition consists mainly of quartz (SiO_2) with a low presence of calcite ($CaCO_3$). We also note the presence of minor mineral phases such as albite ($NaAlSi_3O_8$), orthoclase ($KAlSi_3O_8$) and muscovite (KAl_2 ($AlSi_3O_{10}$) $(OHF)_2$). According to the semi-quantification carried out by X Ray diffraction, the majority clays of the sediment are muscovite and illite-illite interstratified. Chlorite and kaolinite are also observed in smaller proportions. Quartz and calcite are the major non-clays composing the sediment. Different families of feldspars are also present in smaller quantities as well as dolomite in the form of traces. The XRD analysis

Fig. 1. Navigable network of the Nord-Pas de Calais Regional Directorate of Voies navigables de France (VNF-SDRTD, 2009).

Table 2
Characterization of the river sediments.

Characteristics	Standards	Sediment	Normal sand
Density (Kg/m3)	NF EN 1097–7	2610	2650
Methylene blue value (g/100 g of dry matter)	NF P 94–068	0.53	0.50
Organic matter content (%) at 450° C	XP P94–047	4.2	0.1
BET Surface (m^2/g)	NF EN ISO18757	11.0079	–

highlighting the crystallized phases thus proves that this sand consists exclusively of crystallized silica (Quartz) Which corresponds to the very nature of the sand.

The results (Table 3) show that the sediment mainly contains oxygen (O), silicon (Si) and calcium (Ca). Iron (Fe) and aluminum (Al) are present in significant amounts. Several elements are observed at levels close to 1%, this is the case of magnesium (Mg) and potassium (K). Finally, it should be noted the presence of very low levels of sodium (Na), phosphorus (P), and sulfur (S), titanium (Ti) and chlorine (Cl) in the form of traces.

The leaching tests were carried out in accordance with the European standard EN 12457–2: (2002). The principle of the test consists in exposing the crushed material to a leachate during 24 h, and then analyzes the obtained eluate. This test was realized on the fraction of sediment with a particle size less than or equal to 4 mm and was performed in triplicate. A test portion corresponding to 90 g (± 5 g) of dry mass is placed in a one-liter flask. The material of the flask is chosen so as to limit as much as possible the interactions with the waste tested and as a function of the substances assayed during the analysis of the eluate (in our case, it is high density polyethylene). The lixiviate used is ultra-pure water. The amount of leachate to be added is determined so that the liquid / solid ratio (L / S in L / kg of dry matter) is 10 (± 2%). The flask is then shaken with a rotary shaker at 10 rpm for 24 h (± 30 min). At the end of the test, the separation of the eluate from the solid is done in 2 steps. First, the mixture is allowed to settle (for 15 min ± 5 min) and then the eluate is filtered through a 0.45 μm cellulose acetate membrane. A centrifugation step can be added in case of problems. For each eluate, the pH, the conductivity and the temperature are systematically measured. The results of leaching test (Table 5) show that the release in metallic trace elements is respected for all the values of the inert waste thresholds. But against, the sediment is considered as non-inert and non-hazardous waste, according to the decree of 12 December 2014, because the quantity of fluoride released

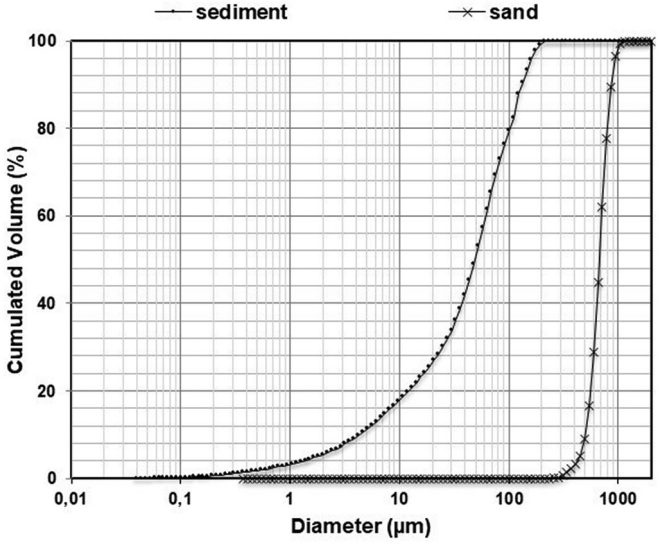

Fig. 2. Particle size distribution of aggregates.

Table 3
Elemental composition in X-ray fluorescence of the sediment.

Elements (%)	O	Na	Mg	Al	Si	P	S	Cl	K	Ca	Ti	Fe
Content	48,5	0,4	0,9	6,7	24,8	0,5	0,4	Traces	1,8	11,8	0,5	3,6

is twice of limit value of threshold. For standardized sand, the results of the batch leaching test (NF EN 12457–2) show that the concentrations of metallic trace elements, anion and soluble fraction are well below the Inert material thresholds (Table 4). Only barium and vanadium could be quantified and it should be noted that the released barium concentration is well below the inert thresholds.

2.3. Mortar manufacturing

As previously indicated, the purpose of using the packing density model is to combine different granular fraction to minimize the intragranular porosity in the mix [43]. This method is presented in the following.

2.3.1. Optimization of the Packing density of mixture

The Packing Density Model (PDM) makes it possible to forecast the real packing density of a mixture noted ϕ present with different classes from the knowledge of the energy to be used, the packing density of each component and the particle size of each component. This model is based on two physical concepts:

The virtual packing density of the mixture ϒ: it is the maximum packing density that can reach a granular stack, if all the grains were stored optimally. In reality, the experimental packing density is inferior to the virtual packing density.

Clamping index (K): is a representative quantity of clamping intensity. The index is infinite so the actual mixing packing density is equal to the virtual packing density.

Once the interactions are known, the dominant class is determined. The virtual packing density of a mixture of n classes is expressed by the formula:

$$\gamma i = \frac{\beta i}{1-\sum_{j=1}^{i-1}\left[1-\beta i+bij\beta i\left(1-{}^{1}/_{\beta j}\right)\right]yj-\sum_{j=i+1}^{n}\left[1-aij^{\beta i}/_{\beta j}\right]yj} \quad (1)$$

γi: virtual packing density when class i is dominant,n: number of classes in the mixture,βi: residual packing density of class i,βj: residual packing

Table 4
the results of leaching of sediment and sand.

Parameters	Sediment	Sand	ISDI threshold	ISDND threshold
As	0,1	< 0,1	0,5	2
Ba	3	0,03	20	100
Cd	0,01	< 0,01	0,04	1
Co	–	< 0,01	–	–
Cr	0,02	< 0,01	0,5	10
Cu	0,6	< 0,02	2	50
Hg	–	< 0,05	0,01	0,2
Mo	0,1	< 0,1	0,5	10
Ni	0,1	< 0,04	0,4	10
Pb	0,1	< 0,02	0,5	10
Sb	0,11	< 0,05	0,06	0,7
Se	0,07	< 0,11	0,1	0,5
Sn	–	< 0,06	–	–
V	–	0,03	–	–
Zn	1	< 0,03	4	50
Chlorides	36	< 10	800	15,000
Fluorides	20	< 5	10	150
Sulfates	270	< 10	1000	20,000
Soluble fraction	2837	358	4000	60,000
pH	8,09	8,98	–	> 6
Conductivity (μS/cm)	264	27,75	–	–

density of class j,yj: volume proportion of class j in the mixture with:

$$yi = \frac{Vi}{\sum_{j=1}^{n} Vj} \quad (2)$$

aij: loosening effect exerted by a grain j in a stack of coarse grains i,bij: wall effect exerted by a large grain i in a stack of fine grains j.

Calculations of the packing density of the sediment are made by precisely fixing the amount of water demand in the mixtures. Measurements were made for each formulation using a Vicat device following the standard procedure specified in the standard NF EN 196–3. Depending on the water demand, the amount of added water needs to allow a needle penetration depth of 6 mm. This amount of water allows a state of normal consistency of the dough, which corresponds to the maximum filling density of the material. The relationship between the maximum packing density and the water demand of a material is given by [44].

$$C = \frac{1000}{1000 + Mv.\frac{Me}{Mp}} \quad (3)$$

where Mv is the density of the powder (kg/m^3) and Me and Mp are the masses of water and powder respectively (kg).

Furthermore, understanding the behaviour of a mixture requires the knowledge of its packing density. Indeed, there is a direct relationship between packing density and porosity. The latter significantly affects the mechanical properties, durability, and water absorption. The relationship between the maximum packing density and the porosity of a material is given by:

$$n = 1 - C \quad (4)$$

where n is the porosity and C is the packing density of the mix.

Measurement of the packing density of sand is made with the shaking table, the test consists of placing a sample of sand in a mould under the constraint of a piston, and to apply to all the mechanical shake causing rearrangement of the grains, and thus compaction of the sample, the measurement is then that of the apparent density of the sample, which makes it possible to calculate the packing density. The packing density is calculated according to the following formula [45].

$$C = \rho a / \rho rd \quad (5)$$

with.ρrd (g/cm3) = real density in the sense of the standard NF EN 1097–6.ρa (g/cm3) = Apparent density of the material.

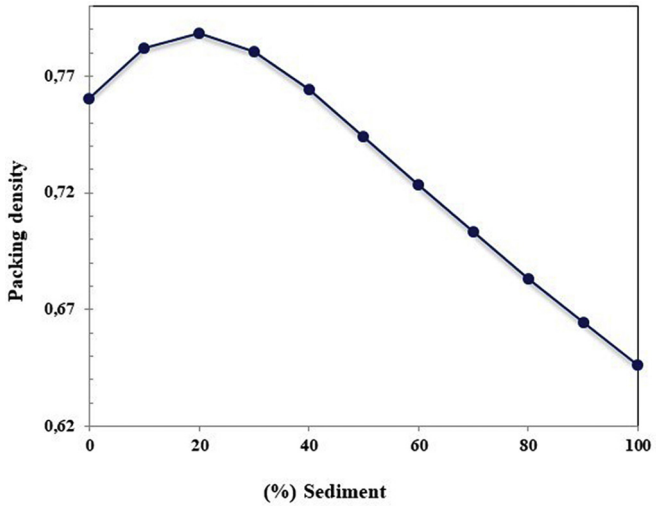

Fig. 3. Evolution of the packing density of the mixtures.

Fig. 3 shows the variation of the packing density of the mixtures as a function of the percentage of the sediment. It is found that the optimal packing density is 0.7885 which correspond of percentage of 20% of the sediment and 80% of the sand. From this curve (Fig. 3) two mixtures were selected for the rest of the study. The first one constitutes 30% sediment and 70% sand, and has a packing density of 0.7805, which is very close to the max value. It was noted PMxSed30. the second one constitutes 50% sand and 50% sediment, and has a packing density of 0.7443. it was noted PMxSed50. For both mixtures the amount of the binder is varied between 12% and 25%. It is found that for the mixture of PMxSed30 the porosity is 21.95% and for the mixture PMxSed50 is 25.57%. Table 5 shows PMxSed30 and PMxSed50 formulations tested. The constituents are stored according to the manufacturer's instructions or the rules of art. The sand was dried at 105 °C for 24 h and the sediment at 60 °C for >72 h to reduce the moisture content. After drying the sediment, it was necessary to crush it and sift it in 2 mm sieve. The resin was stored in a temperature-controlled room. The base product was mixed with the hardener in a first bucket for 3 min until a uniform mixture was obtained. In a second bucket, the charges based on sand and sediment were mixed. The binder was inverted into a second container and knead again for 6 min. Than the mineral charges were added to the binder in 2 parts. Finally, the molds are filled in two layers, and each layer is compacted using the impact table (60 shots). The polymer concrete samples were demolded after 24 h and cured in air at 25 °C and 48% RH.

2.4. Experimental tests

2.4.1. The apparent density

It is defined as the density of one cubic meter of the material comprising the voids of the particles as well as those between particles. The apparent density of a granular material depends on its degree of compaction. It is expressed by the following relation $\rho = M_s/V_t$ where V_t is the total volume and M_s its dry mass.

2.4.2. Mechanical tests

To evaluate the strength of the polymer mortar, unconfined compression (UCS) and three-point bending tests were performed on 40 × 40 × 160 mm samples, according to the requirements of standard NF EN 196–1. Polymer mortar were conserved at a temperature of

Table 5
Polymer mortar formulations.

Formulation	Epoxy resin (kg)	Sand (kg)	Sediment (kg)	Resin content in the mix. (%)
PM12	0.42	3.5	0	12
PM14	0.49	3.5	0	14
PM16	0.561	3.5	0	16
PM18	0.63	3.5	0	18
PM20	0.7	3.5	0	20
PM25	0.875	3.5	0	25
PM12Sed30	0.42	2.45	1.05	12
PM14Sed30	0.49	2.45	1.05	14
PM16Sed30	0.561	2.45	1.05	16
PM18Sed30	0.63	2.45	1.05	18
PM20Sed30	0.7	2.45	1.05	20
PM25Sed30	0.875	2.45	1.05	25
PM12Sed50	0.42	1.75	1.75	12
PM14Sed50	0.49	1.75	1.75	14
PM16Sed50	0.561	1.75	1.75	16
PM18Sed50	0.63	1.75	1.75	18
PM20Sed50	0.7	1.75	1.75	20
PM25Sed50	0.875	1.75	1.75	25

PMx: Polymer mortar with x the polymer content in (%) given by the total weight of the loads.
PMxSedy: Polymer mortar with:
X the polymer content in (%) given by the total weight of the loads.
Y the sediment content in (%) given by the total weight of the loads.

20 °C ± 2 °C and relative humidity maintained at 50% at least. The compression tests were carried out with a load increase of 2400 N/s ± 200 N/s. The three-point bending tests were performed with a speed loading of 50 N/s ± 10 N /s. Otherwise the dynamic modulus of elasticity has also been measured by Grindo-sonic frequency analyzer on 40 × 40 × 160 mm specimens.

2.4.3. Porosity

Porosity by mercury intrusion was measured using mercury porosimetry. This technique provides rapid access to pore distribution with good accuracy in the range of 3 nm to 360 μm and the mercury pressure range is 30,000 psi (206 MPa).

2.4.4. The absorption of water

The absorption of water is followed over time by simple gravimetric measurement. The formula for calculating the mass gain is:

$$gain\ mass\ (\%) = \frac{M(t) - M(0)}{M(0)} * 100$$

where M(t) is the mass of the MBR after immersion for a time "t" and M (0) the initial mass of the specimen in the dry state.

2.4.5. Linear thermal expansion

The experimental tests were carried out in accordance with standard NF EN ISO 10545-8 on three test pieces of each formulation. The samples were dried at a constant temperature (110 ± 5 °C) to constant mass and then introduced into a desiccator to cool to room temperature.

2.4.6. The thermal shock resistance test

Was carried out on three samples (80 mm × 40 mm × 40 mm) of each formulation. The specimen subjected to 10 cycles during which the temperature varies between 15 °C and 145 °C. according to EN ISO 10545-9. The visible defects on the specimens were identified by examining them with the naked eye.

2.4.7. The chemical resistance

Test was carried out in accordance with EN 10545–13. The following solutions were used:

- 3% hydrochloric acid solution (volumetric percentage).
- 18% hydrochloric acid solution (volumetric percentage).
- Potassium hydroxide (KOH) solution, 30 g / l.
- Potassium hydroxide (KOH) solution, 100 g / l.

The test specimens were immersed in the citric acid solution and kept in the laboratory for 24 h according to the standard. For the hydrochloric acid and potassium hydroxide resistance test, the specimens were immersed for 96 h.

3. Results and discussion

3.1. The apparent density

The Fig. (4a) shows the evolution of Polymer mortars PMx density for the curing time of 7, 14 and 28 days. We note that the density was range between 1689.23 kg / m3 and 1891.12 kg / m3. The increase in the density observed during the curing time for the polymer mortar (PMx) can be attributed to the increase of the crosslinking density of the epoxy polymer binder, which already related in a previous study on the micro epoxy concrete polymer [46]. At 28 days of curing, it is noted that the density of the polymer mortar increased by 1.28% for the mass fraction of the binder range from 12% to 14% and then decreases by 2.38%, 3.68%, 1.01%, 2.33% and 0.63% respectively when the mass fraction of the binder increases between 14% and 25%. There is an optimum of resin quantity (14%) which makes it possible to have a maximum density of PMx mortars. This can be explained by the fact of increasing the mass fraction of the resin (density equal to 1100 kg/m^3) implies a decrease in the granular mass fraction (density equal to 2600 kg/m^3), causing a decrease in the density of the mixture. The graph (4-b) and (4-c) shows the evolution of polymer mortars density PMxSed30 and PMxSed50 for 7 days, 14 days, and 28 days. At 28 days curing time, the density of all mixtures incorporating sediment was range between 1500 kg/m^3 and 2000 kg/m^3. It is noted that the density decreases in day 14 except for the PM16Sed30 and PM20Sed30 formulations. It is noted that the density decreases in day 14 except for the PM16Sed30 and PM20Sed30 formulations. Unlike polymer mortars without sediments (PMx), the density increases with the increase in the mass rate of sediments. It is observed that the density for the formulations PM12Sed50 and PM14Sed50 is decreased to 1.45% and 3.57%, for PMxSed50 for x equal 18 and 25 increased by 1.87% and 1.63% respectively. It is observed that the density of the polymer mortar (PMxSed50) at 28 days bound to the mass fraction of the binder. Fig. 5 shows the density of polymer mortars at 28 days. We note that the density of the PMx polymer mortar for the mass fraction is 12, 14 and 16% are higher than that of the polymer mortar PMxSed30 and PMxSed50. The mass fractions of the binder equals 18% and it is observed that the density of the PMx polymer mortar is low compared to PMxSed30. It is observed that the density is related to the amount of binder and sediment. From the 16% of the mass fraction of the binder, the density of the polymer mortar PMx decreases, unlike the polymer mortars based on the sediment. For comparative purposes, several study [33,39,41,47], where they optimized the polymer mortar or concrete, showed that the incorporation of fillers (marble powder, cork granules, sand) increased the density of polymer concrete until some mass fractions of the binder which causes a drop in the latter.

3.2. Compressive test

Figure (Fig. 6a) shows the evolution of the compressive strength of the PMx formulation for 7 days, 14 days and 28 days. All the test results were calculated by the average of three measurements for each type of samples. It's notes that the compressive strength increases for all mass fractions of resin as a function of time. It is observed that between 7 days and 28 days will not have much difference in compressive strength. Several studies [48–50] shown that the compressive strength of the polymer concrete becomes almost constant and that it reaches three-thirds of its maximum compressive strength in the first days of curing. It is observed that compressive strength increases when the content of the binder increases between 12 and 18%. Hereafter 18% of binder content the compressive strength decreases gradually. This can be explained by fact that appearance of saturated zone with epoxy binder, which decreases intragranular interaction and deteriorate consequently the mechanical properties of the mortar PMx. The Fig. 6b shows the evolution of the compressive strength of the PMxSed30 formulation for different percentages of mass fraction for 7 days, 14 days and 28 days. It is noted that compressive strength increases over time for all PMxSed30 formulations except for the PM18Sed30 formulation. It notes that the compressive strength of the polymer mortar PMxSed30 increases as the amount of resin content increases. It is observed that the compressive strength is almost stable for 28 days. Note that the compressive strength between the mortar PM16Sed30 and PM18Sed30 increases by 118%. This can be mainly due to the reduction of the internal porosity of the polymer mortars. In fact, it is noted that the porosity decreases from 15% to about 5% between the mortars PM16Sed30 and PM18SED30, respectively. Fig. 7 shows the compressive strength of the mortars PMx, PMxSed30 and PMxSed50 in 28 days, we take note that:

- The compression strength of masse fractions equal to 12; 14; 16; 18; 20 and 25 of the PMxSed30 formulation is small compared to the

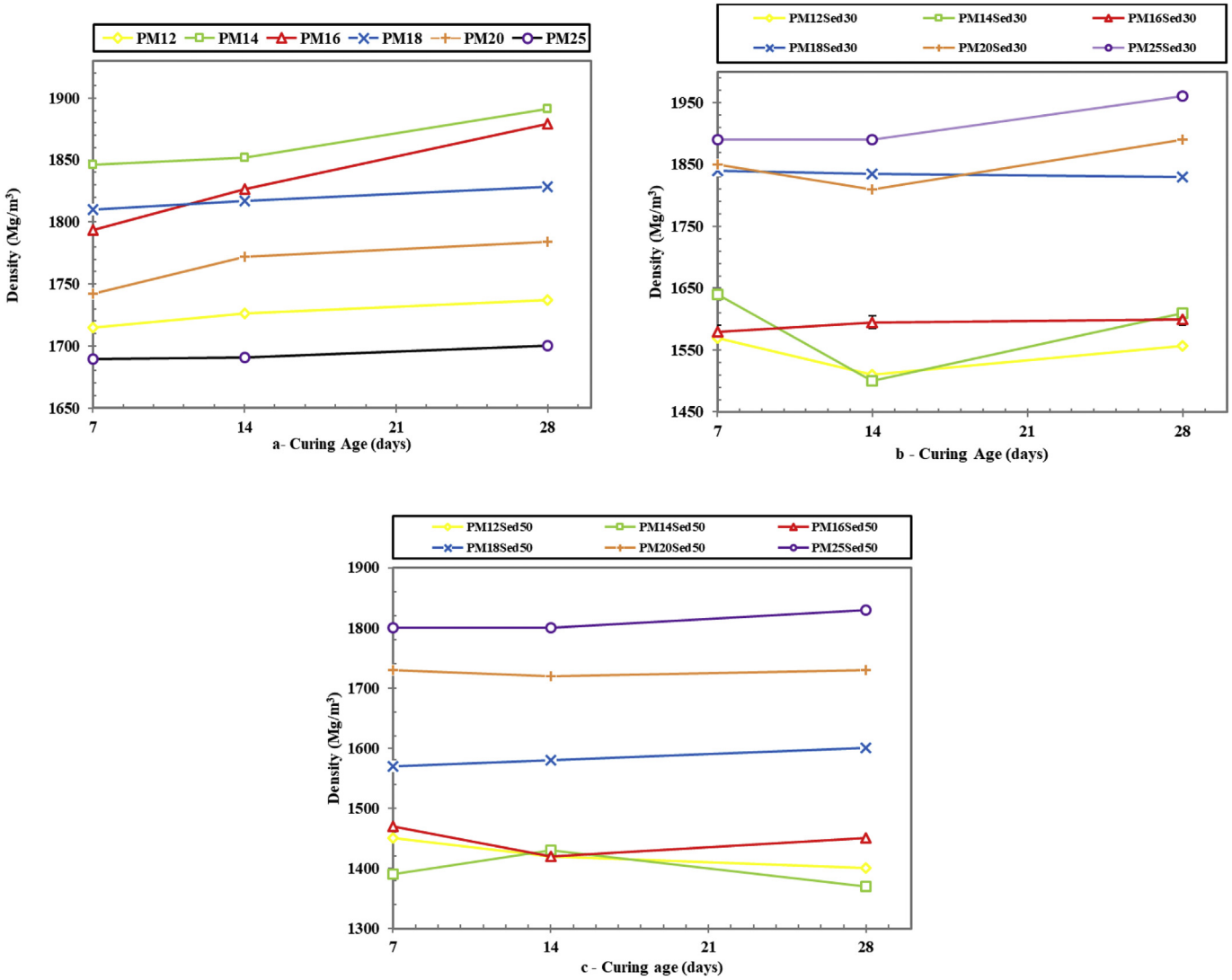

Fig. 4. (a) (b) (c) evolution of the density of PMx and PMxSed30, PMxSed50 respectively, as a function of curing age.

mortar PMx of the same mass fraction with a percentage difference of 74.59%, 75.89%, 67.11%, 33.86%, 20.14% and 3.32%, respectively.

- The compression strength of masse fractions equal to 12, 14, 16, 18, 20 and 25 of the PMxSed50 formulation is small compared to the mortar PMx of the same mass fraction with a percentage difference of 89.9%, 92.2%, 84.65%, 74.53%, 42.51% and 11.51%, respectively.
- The compression strength of masse fractions equal to 12; 14; 16; 18; 20 and 25 of the PMxSed50 formulation is lower compared to the mortar PMxSed30 of the same mass fraction with a percentage difference of 52.03%, 67.68%, 53.33%, 61.49%, 28.02% and 8.47%, respectively.

These differences can be expressed by several factors by the lack of the amount of binder required to coat the aggregates and fill the voids between the aggregates. The increase in the binder content allows a better coating of the aggregates and leads to completely filling the gaps between the aggregates. Several previous study [36,51–53] confirm these observations. Indeed, it is observed that the compressive strength decreases when the amount of the sediment increases, and the amount of fines affects the mechanical properties from the amount added to the matrix. Another explanation for this decrease can be due to a high capacity to absorb water. In fact, during the mixing with the resin, sediments absorbed a certain quantity of the resin. Several studies have shown the influence of granulometry on the properties of the polymer mortar also as reported in the literature [54]. The granular mixture in

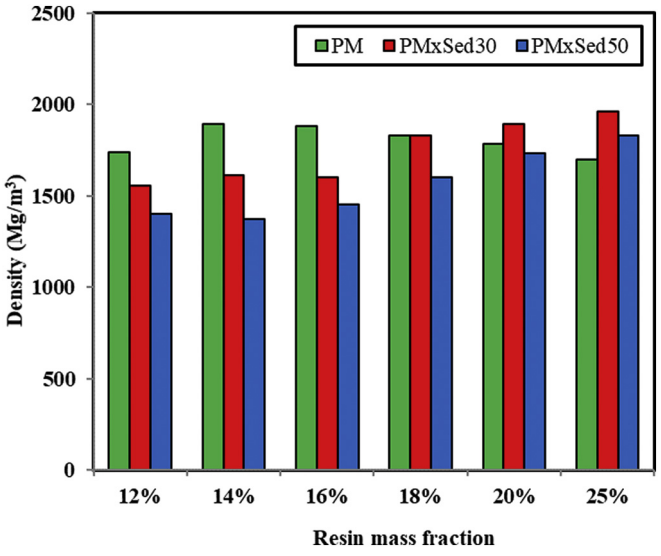

Fig. 5. Comparison between different densities of mix at 28 days.

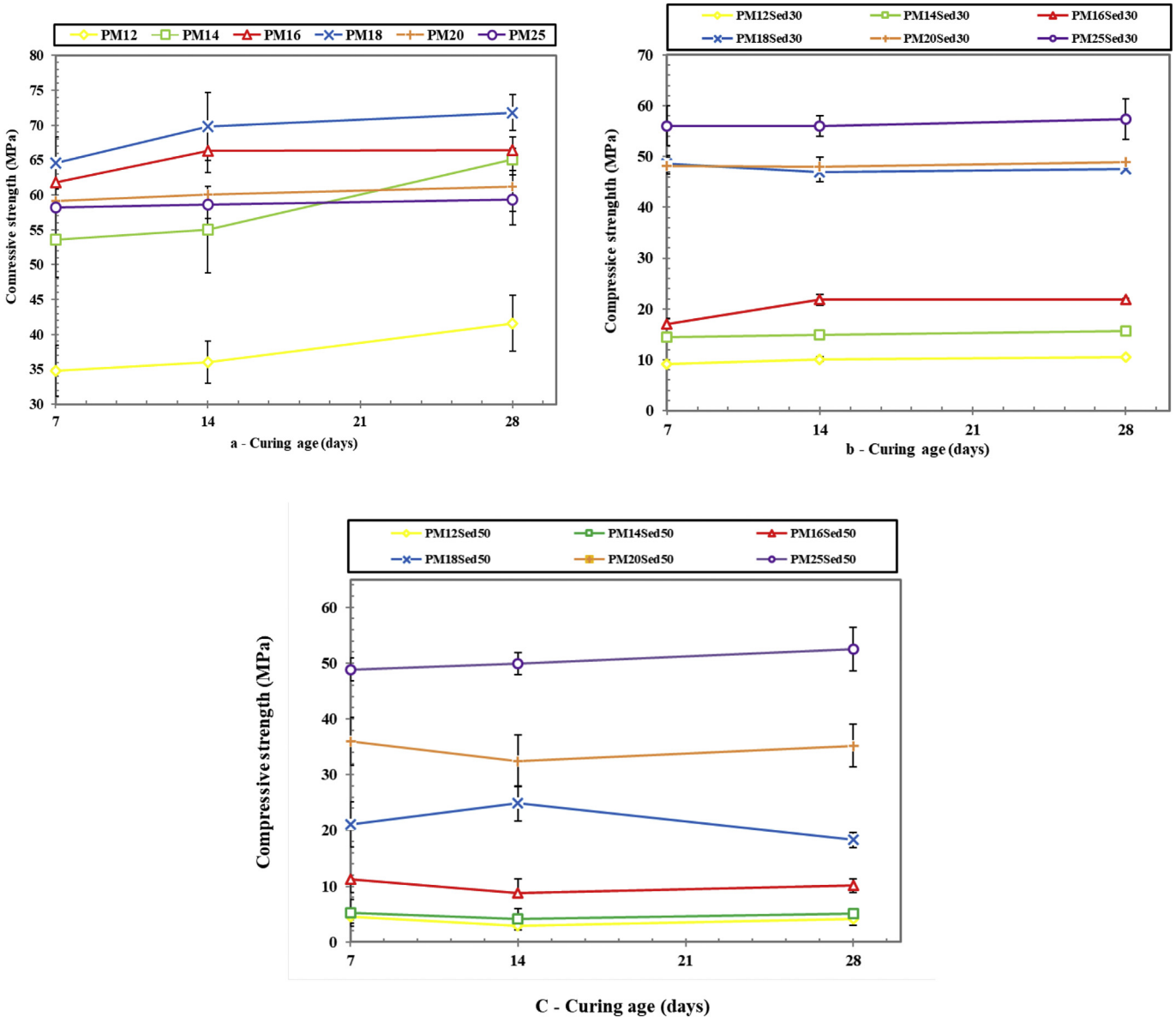

Fig. 6. (a), (b), (c) show the evolution of the compressive strength of PMx and PMxSed30, PMxSed50 respectively, versus curing age.

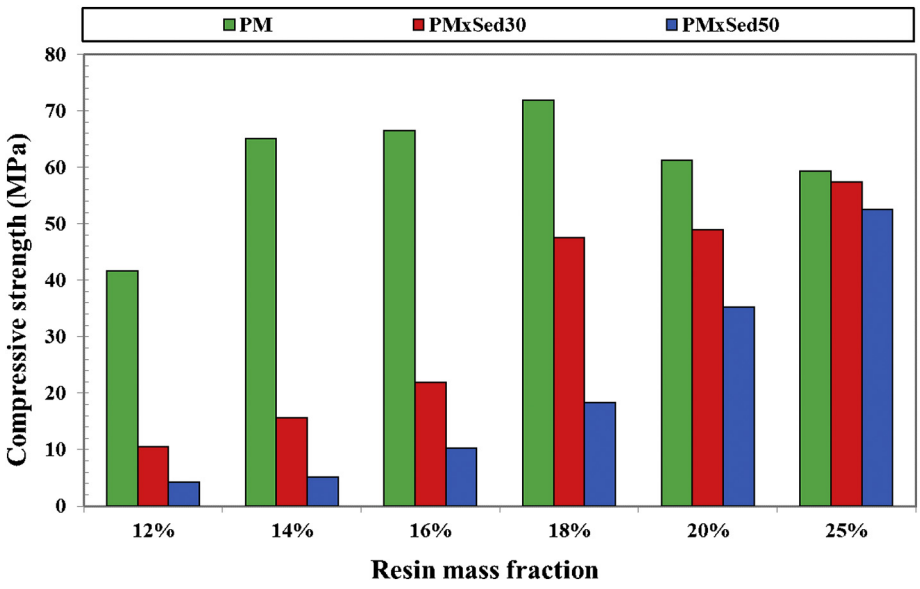

Fig. 7. Compressive strength of PMx, PMxSed30 and PMxSed50 versus resin mass fraction.

the mortar affects the compressive strength. The granular mixture must be mixed in a manner and a minimum void content and maximum bulk density [55]. The smaller particles have a larger area. Therefore, the specific area of the sediment is larger compared to the sand implies a higher dosage of resin. in the literature [56–58] has shown the effect of the specific surface area on the amount of resin and on the compressive strength. This difference in compressive strength between mortars can be explained by the difference in the type of aggregates. Indeed, Fu et al. [53] has shown that the type of aggregates affect compressive strength. The bond between the charge and the matrix and the amount of charges in the matrix are two important factors that also affect the mechanical properties [53]. For well-matrix-bound fillers, the stress applied to the mortar can be efficiently transferred to the particles from to the matrix.

3.3. Flexural strength

The Fig. (8a, b and c) shows the flexural strength of the mortar PMx, PMxSed30 and PMxSed50 formulation of different resin mass fractions for 7 days, 14 days and 28 days. For the PMx formulations, it is observed that the resistance increases with time for all the mass fractions. It should be noted that flexural strength increases with the increasing resin content. By 25% of the mass fraction of the resin, the flexural strength decreased slightly. The flexural strength of the PMx mortar increased by 54.11% as the mass fraction of the binder increased from 12% to 14%. From the mass fraction, 14% the flexural strength between 20.59 MPa and 25.89 MPa. At 28 days, the flexural strength of 4.8 MPa to 7.96 MPa was observed for the PM12Sed30, PM14Sed30 and PM16Sed30 mortars. For mortars PM18Sed30 and PM20Sed30, the flexural strength is between 16.89 MPa and 18.03 MPa. For mortar PM25Sed30 is 26.03 MPa. Otherwise, at 28 days, the flexural strength of PM12Sed50, PM14Sed50, PM16Sed50, PM18Sed50, PM20Sed50 and PM25Sed50 equals 1.71 MPa, 4.65 MPa, 4.93 MPa, 8.91 MPa, 11.94 MPa and 20.05 MPa respectively. It is observed that for all formulations (PMx, PMxSed30 and PMxSed50) the flexural strength is related to the resin content. Fig. 9 shows the flexural strength of the formulations: PMx; PMxSed30 and PMxSed50 in twenty-eight days. it is found that the flexural strength of PMx is greater than that of PMxSed30 and PMxSed50 formulations for a mass fraction equal to: 12; 14; 16; 18 and 20%.

It follows from the foregoing it is noted that:

- The flexural strength of mass fraction equal to 12; 14; 16; 18; 20 and 25% of the PMxSed30 formulations decreased by 64.07; 67.45; 66.12; 28.97 and 30.35% compared to the PMx formulation respectively.
- The flexural strength of mass fraction equal to 12; 14; 16; 18; 20 and 25%of the PMxSed50 formulation decreased by 87.20; 76.05; 62.53; 28.97, 53.88 and 20.75% compared to the PMx formulation respectively.

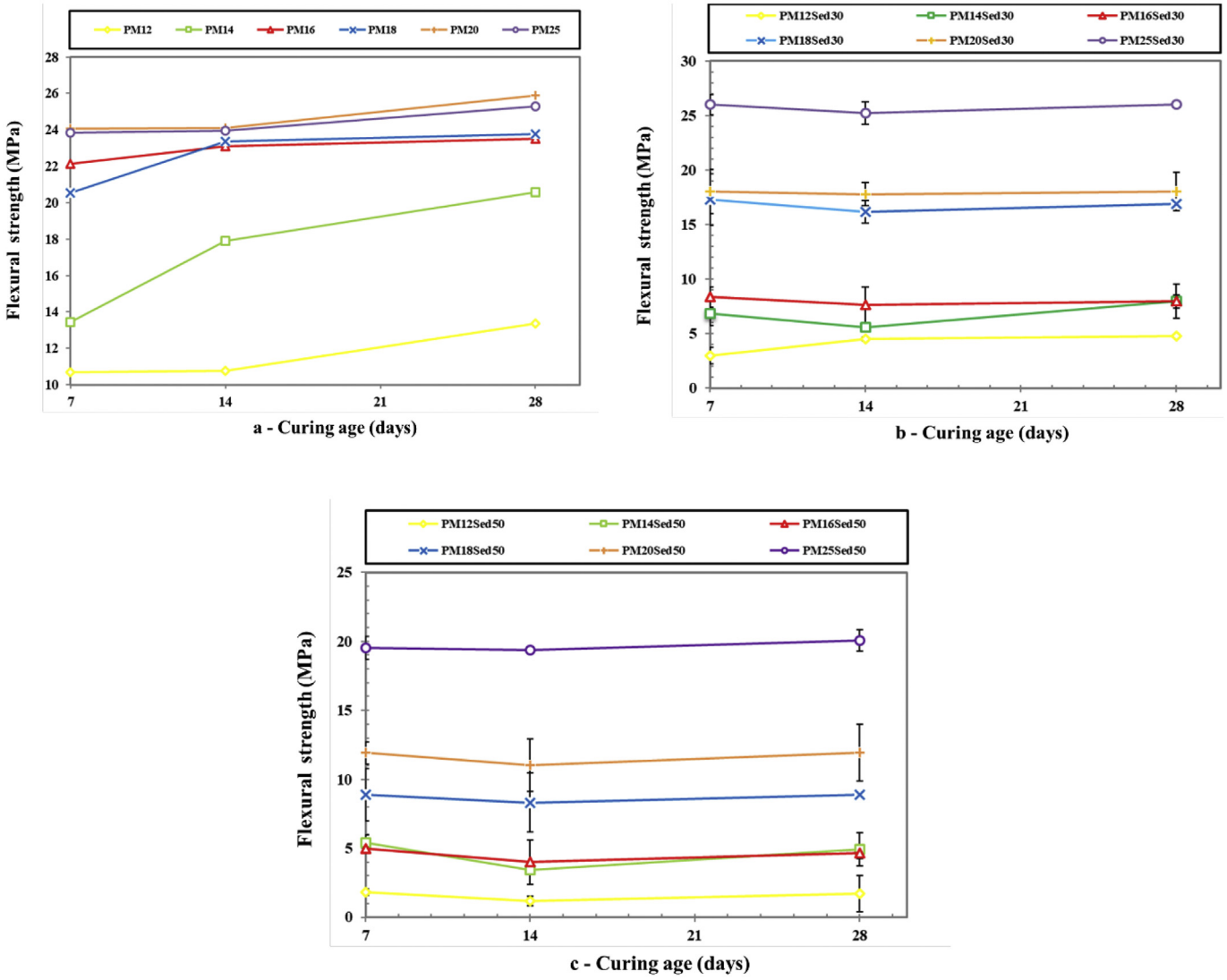

Fig. 8. (a), (b), (c) show the evolution of the flexural strength of PMx and PMxSed30, PMxSed50 respectively, versus curing age.

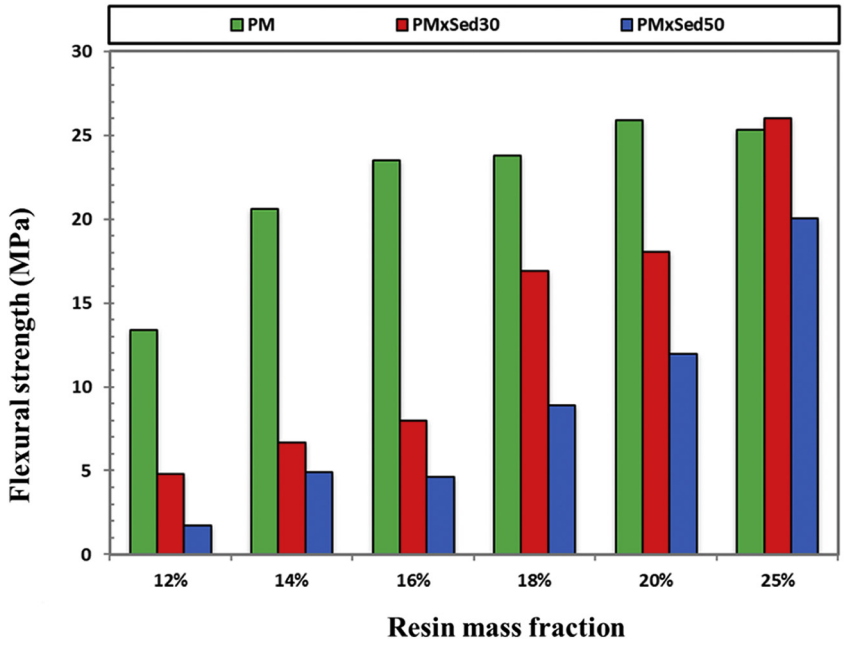

Fig. 9. Flexural strength of PMx, PMxSed30 and PMxSed50 versus mass fraction of resin.

- The flexural strength of the mass fraction equal to 12; 14; 16; 18; 20% and 25 of the PMxSed50 formulation decreases by 53.88; 26.41; 41.58; 47.24; 33.77 and 22.97% compared to the PMxSed30 formulation respectively.

Several factors affect flexural strength, such as the amount of resin, the nature and amount of the filler and the particle size of the filler. In a research article [58], they arrived at the same results. The flexural strength of the polymer mortars PMx and PMxSed30, PMxSed50 can be related to the mass percentage of the resin by a linear relationship of positive slope with a correlation of 0.76 and 0.92, 0.92 respectively.

3.4. Modules of elasticity

The Fig. 10 shows the modulus of elasticity of the mortars PMx, PMxSed30 and PMxSed50as a function of the mass fractions. The modulus of elasticity of the PMx mortar decreased by 10.05% for mass fraction between the ranges of 16% to 25% there is an increase of 29.49% for mass fraction between 12% and 18%. It is observed that the modulus of elasticity of the PMxSed50 formulation is increased from 1.45 GPa to 11.9 GPa when the mass fraction increases from 12% to 25%. For the equal mass fraction 20, the modulus of elasticity of the mortar PMxSed30 slightly exceeds the modulus of elasticity of the PMx mortar. The modulus of elasticity of the mortar polymer PMxSed30 is higher than that of the modulus of elasticity of the mortar PMxSed50, the

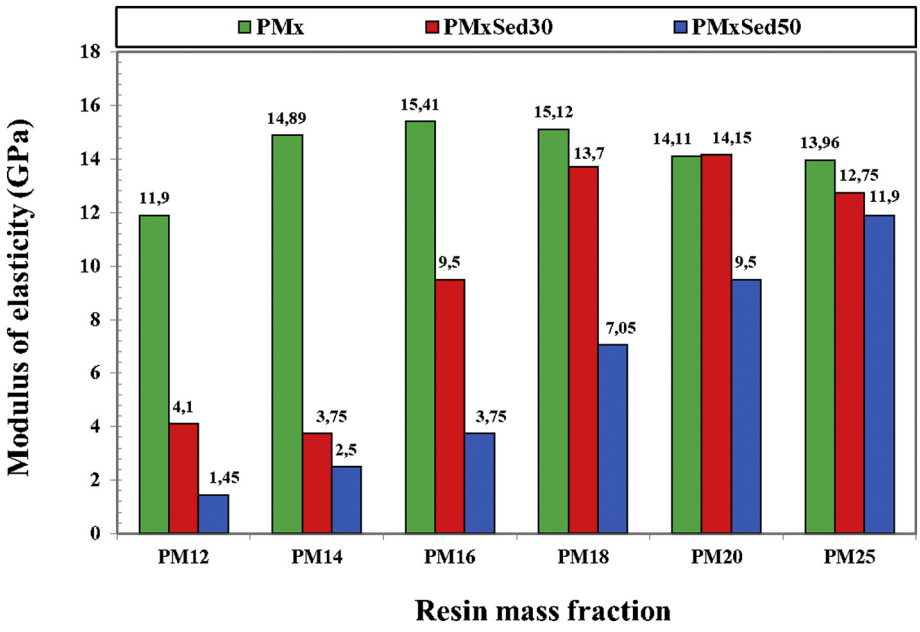

Fig. 10. Modulus of elasticity of PMx, PMxSed30 and PMxSed50 versus mass fraction of resin.

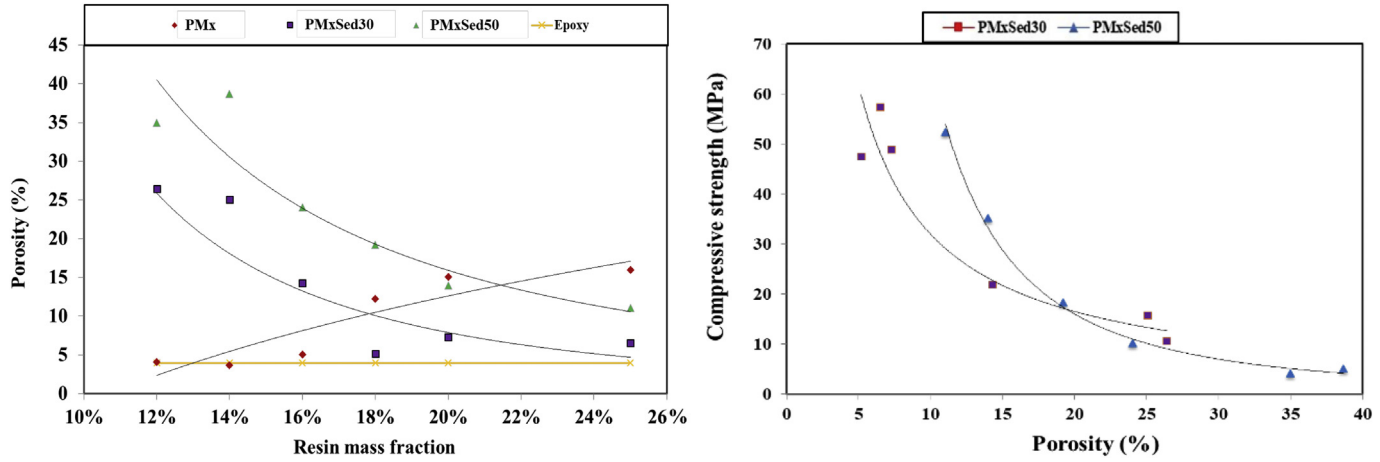

Fig. 11. (a) Evolution of the porosity of the mortar PMx, PMxSed30 and PMxSed50 versus resin mass fraction; (b) the compressive strength as a function of the porosity.

difference percentages is 64.63; 34.21; 60.52; 48.54; 32.86 and 6.66 for the equal weight fraction 12; 14; 16; 18; 20 and 25% respectively.

It is observed that the modulus of elasticity is related to the mass fraction of the resin, the modulus of elasticity can be related to the mass fraction of the binder with a linear function of the positive slope with a strong correlation of 0.79 and 0,97 for PMxSed30 and PMxSed50 formulations respectively. For the PMx formulation have a low correlation of 0.10. It is concluded that the modulus of elasticity of the polymer mortar PMxSed30 and PMxSed50 increases when the quantity of the resin increases unlike the mortar PM it reaches the optimum value (the mass fraction equal to 16%). The amount of sediment increases the modulus of elasticity decreases. This phenomenon can be explained by the particle size of the sediment that affects the charge distribution in the matrix. The nature of the sediment being different from that of sand, this difference influences the modulus of elasticity, which confirms in the literature [59,60]. The interfacial load / matrix has an important role on the modulus of elasticity [61]. The bond of the sand with the resin is different from the bonding of the sediment with the resin the adhesion force corresponds to the chemical reactions between the load and the resin which this reaction depends on the elements that make up the load.

3.5. Porosity

The Fig. 11a shows the porosity of the mortar PMx, PMxSed30 and PMxSed50 as a function of the mass fraction. The value of the porosity of epoxy resin without charge is equal to 3.95% this porosity can be related to the binder preparation, during the mixing air balls were observed where it can be related to the pressure exerted by the mercury porosimetry on the composite. Note that the porosity of the PMx mortar decreases when the mass fraction of the resin increases from 12% to 14%, the porosity increases by 68.43% when the mass fraction increases from 14% to 25%, the same phenomenon observed in the study [33]. This phenomenon can be explained by the study of [62], the fact that the apparent absorption of mercury by the polymer mortar fills the void in the material produced by the collapse or compression of the material and that the material has a restitution or elasticity and resumes its original shape or volume. But it is observed that 100% of the resin content that the porosity lower than the porosity of the polymer mortar, can explain this difference by the fact that the mercury pressure applied to the charges leads to applying a force on the matrix, which implies a deformation on the opens the pores.

The PMxSed30 mortar porosity value decreased by 80.38% when the resin mass fraction ranging from 12% to 18%, and increases of 25.67%, when the resin mass fraction range from 18% to 25%. It is noted that the value of the porosity of the mortar PMxSed50 is increased by 10.6% between the mass fraction of 12% to 14%, after the mass fraction of 14%, the porosity decreases with a percentage of 71, 43%. The porosity of the PMxSed30 and PMxSed50 mortars related to the mass fraction by a relationship of negative slope. With regard to the PMx mortar, the porosity can be related to the mass fraction by a linear relationship of positive slope with a correlation equal to 0.88. The value of the porosity of the mortar PMx is large compared to the value of the porosity of binder; it is observed that the percentage difference in value of the porosity between the mortar PMx and the binder increases with the increase of the mass fraction. Contrary for the mortar PMxSed30 and PMxSed50 the value of the porosity becomes close to the value of the porosity of binder with the increase of the mass fraction.

It is noted that over the mass fraction range of 12% to 25% the value of the porosity of the mortar PMxSed50 is greater compared to the mortar PMxSed30. This difference can be explained by the amount of sediment increases implies that the adhesion force between the load and the matrix is low; this weakness leads to empty spaces. Sediments characterizations have a role on the porosity, the percentage of water absorption of the sediment is important which leads to the absorption of the resin by the sediment until saturation.

The Fig. 11b shows the curve of the compressive strength as a function of the porosity. Note that the compressive strength of the mortar PMxSed30 and PMxSed50 decreases when the porosity increases which is equivalent to a decrease in the mass fraction of the binder. But the compressive strength of the mortar PMx is not related to the porosity so that a weak correlation of 0.07. The compressive strength of the mortar PMxSed30and PMxSed50 can be related to the porosity by a linear relationship of negative slope with a correlation of 0.88 and 0.79, respectively.

3.6. Water absorption

Fig. 12a illustrates the evolution of water absorption of the PMx mortar with different mass fractions of the binder as a function of time. It should be noted that PMx water absorption decreases as the mass fraction of the binder decreases. It should be noted that the PMx mortars are saturated from 4 h except the PM12 mortar. Fig. 12b illustrates the evolution of the water absorption of the PMxSed30 mortar with different mass fractions as a function of time. It should be noted that the water absorption of PMxSed30 decreases as the mass fraction of the binder decreases. Mortars PM12Sed30, PM14Sed30 and PM16Sed30 saturate after 12 h, unlike mortars PM18Sed30, PM20Sed30 and PM25Sed30. The Fig. 12c illustrates the evolution of the water absorption of the mortar PMxSed50 with different resin mass fractions as a function of time. It noted that the water absorption of PMxSed30 decreases as the mass fraction of the binder decreases. PM12Sed50, PM14Sed50 and PM16Sed50 mortars saturate them from 12 h unlike PM18Sed50, PM20Sed50 and PM25Sed50 mortars. Water absorption increases as the percentage of

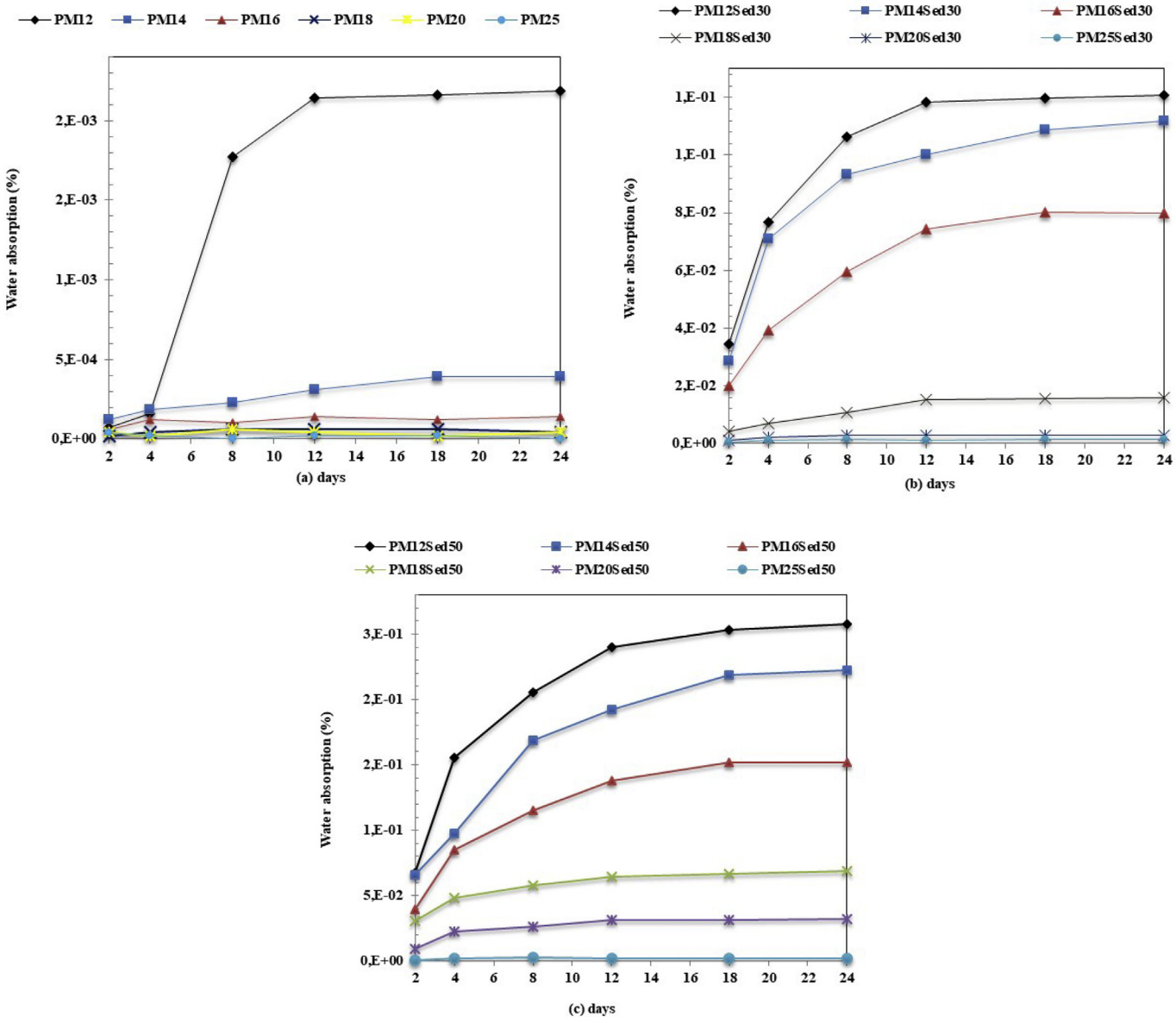

Fig. 12. (a), (b) and (c) the water absorption of the PMx and PMxSed30, PMxSed50 mortar respectively as a function of curing time.

sediment increases and the mass fraction of the binder decreases. In the literature [63] they confirmed the relationship between resin quantity and water absorption. The resin covering the charges prevents the penetration of water; when the amount of resin is insufficient to cover the entire charge the water penetrates remains stuck in the mortar where the charges of the unsaturated sediment absorb it.

3.7. Linear thermal expansion

The Fig. 13 shows the evolution of the coefficient thermal expansion of the PMx, PMxSed30 and PMxSed50 mortars as a function of the mass fractions, we observe that:

- The graph of the thermal expansion of the PMx mortar is an increasing curve, the thermal expansion increases as the mass fraction increases. The value of the thermal expansion is increased by a percentage of 33.33%; 37.49%; 38.7%; 18.6%; between the mass fraction of 12% to 14%; 14% to 16%; 18% to 20% and 20% to 25% respectively and a slight decrease of 6.06% between the mass fraction of 16% to 18%. The thermal expansion curve of the PMx mortar can be connected to the mass fraction by a linear relationship of positive slope with a correlation of 0.94.
- The thermal expansion curve of the PMxSed30 mortar is an increasing curve as a function of the mass fractions. It is observed that between the intervals of the mass fraction comprised between 12% to 14%; 16% to 18%; 18% to 20% and 20% to 25%, the value of thermal expansion increases by a percentage of 36.36; 78.57; 27.99 and 21.87 respectively. For the interval between 14% and 16%, the value of the thermal expansion reduces by 6.66%. The thermal expansion curve of the PMxSed30 mortar can be related to the mass fraction by a linear relationship of positive slope with a correlation of 0.93
- The thermal expansion curve of the mortar PMxSed50 is increasing as a function of the mass fraction of the binder, it is found that the value of the thermal expansion increases by a percentage of 175; 63.63; 27.77 and 17.39% between the mass fractions of 14% to 16%; 16% to 18%; 18% to 20% and 20% to 25% respectively. Between the mass fractions of 12% to 14% decreases by 20%. The thermal expansion curve of the PMxSed50 mortar can be connected to the mass fraction by a linear relationship of positive slope with a correlation of 0.91

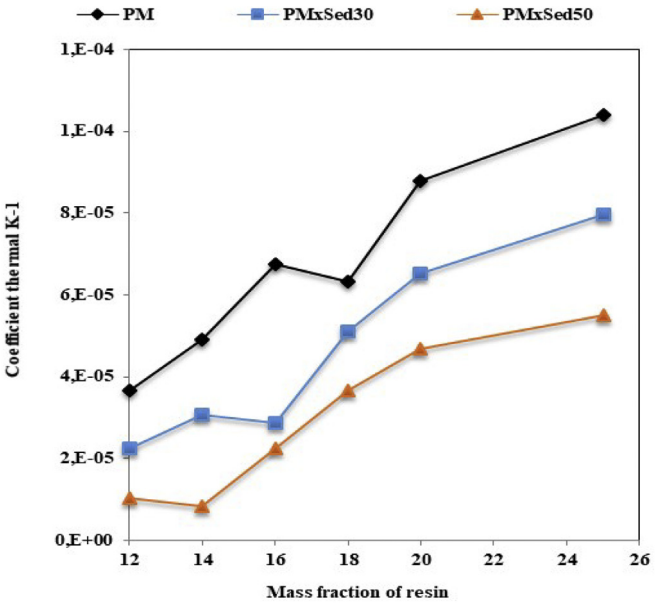

Fig. 13. Evolution of the coefficient of thermal expansion of the PMx, PMxSed30 and PMxSed50.

The coefficient of thermal expansion of epoxy mortars is higher; the thermal expansion coefficient increases as the amount of resin increases and the coefficient of thermal expansion decreases when the load increases even remarks reported in a paper search [64]. These results can be explained by the connection between the charge and the matrix; when the important bond the coefficient thermal expansion is high. The type and shape of the load influences the thermal expansion coefficient we note that the thermal dilation coefficient of PMx is different from PMxSedy, in the literature have shown that the nature of charge [65] and the shape [66].

3.8. The thermal shock resistance

From visual examination according to the conditions of the standard on a surface treated with methyl blue, the modifications observed are small cracks and exfoliations on PM12Sed30 and PM12Sed50 formulations; these modifications can be explained by the low resin content which leads to a weak bond between the fillers and the matrix; for other formulations no modification. In a paper search [31], they did not observe modifications for a polymer mortar with a mass fraction of 30% epoxy and 70% of fillers (crushed granite).

3.9. Chemical resistance

It was noticed that the PM12 Sed30 and PM12 Sed50 and PM14 Sed50 formulations are not resistant to the attacks of the solutions (KoH and Hcl). Modifications have been observed on the surface of the tested samples and that the solutions attack the load, these attacks related to the small amount of resin that covers the charges. In the researches [67,68] have tested several chemical solutions on epoxy mortars. They concluded that epoxy mortars are resistant to chemical attack.

3.10. Leaching test of crushed samples

The Table 6 shows the results of the leaching of the PMxSed30 mortar of the different mass fractions of binder. It is noted that for PMxSed30 mortar of different mass fraction the leaching result shows that the value of the antimony element (Sb) is exceeded the threshold. The soluble fraction value of the mortar PM18Sed30, PM20Sed30 and PM25Sed30 exceeds the threshold. It should be noted that the values of the chemical elements of the PMxSed30 mortar are less than or equal to the values of the raw sediment. The fluoride value of the raw sediment is exceeded the threshold but after the incorporation of the sediment in a polymer matrix this value has decreased and the more the mass fraction of the binder increases this value decreases. The pH of the PMxSed30 mortar is almost stable and its value between the pH value of the sediment and the value of the sand. The soluble fraction increases with the increase of the mass fraction of the binder. The conductivity of the PMxSed30 mortar is small compared to the raw sediment but it is large compared to the sand. The PMxSed30 mortar of the different mass fraction of the binder is a non-inert and non-hazardous mortar. The Table 7 shows the results of the leaching of the PMxSed50 mortar of the different mass fractions of binder. It is noted that for **PMxSed30** mortar of different mass fraction the leaching result shows that the value of the antimony element (Sb) is exceeded the threshold. The value of the soluble fraction of PMxsed50 mortar for all mass fractions of binder exceeds the thresholds. It should be noted that PMxSed50 mortar chemical values are less than or equal to raw sediment values. The fluoride value of the raw sediment is exceeded, but

Table 6
Results of leaching tests of mixtures PMxSed30.

Parameters	Sediment	Sand	PM12 Sed30	PM14 Sed30	PM16 Sed30	PM18 Sed30	PM20 Sed30	PM25 Sed30	ISDI threshold	ISDND threshold
As	0,1	< 0,1	0,11	< 0,09	0,12	0,11	0,12	0,15	0,5	2
Ba	3	0,03	< 0,007	0,01	0,01	0,03	0,02	0,02	20	100
Cd	0,01	< 0,01	< 0,02	< 0,02	–	< 0,02	< 0,02	< 0,02	0,04	1
Co	–	< 0,01	0,14	0,12	0,11	0,16	0,26	0,17	–	–
Cr	0,02	< 0,01	< 0,004	< 0,004	–	< 0,004	< 0,004	< 0,004	0,5	10
Cu	0,6	< 0,02	< 0,007	0,07	–	< 0,007	< 0,007	< 0,007	2	50
Mo	0,1	< 0,1	< 0,04	< 0,04	–	< 0,04	< 0,04	< 0,04	0,5	10
Ni	0,1	< 0,04	< 0,03	< 0,03	–	< 0,03	< 0,03	< 0,03	0,4	10
Pb	0,1	< 0,02	< 0,09	< 0,09	–	< 0,09	< 0,09	< 0,09	0,5	10
Sb	0,11	<0,05	< 0,2	< 0,2	–	< 0,2	< 0,2	< 0,2	0,06	0,7
Se	0,07	< 0,11	< 0,1	< 0,1	–	< 0,1	< 0,1	< 0,1	0,1	0,5
Sn	–	< 0,06	< 0,09	< 0,09	–	< 0,09	< 0,09	< 0,09	–	–
V	–	0,03	0,08	0,07	0,08	0,08	0,09	0,09	–	–
Zn	1	< 0,03	< 0,01	< 0,01	–	< 0,01	< 0,01	< 0,01	4	50
Chlorides	36	< 10	< 10	12,5	15	30,5	36,5	24	800	15,000
Fluorides	20	< 5	7,25	5,7	4,05	4,15	4,3	4,55	10	150
Sulfates	270	< 10	83,5	74,5	112,5	140	149,5	130,5	1000	20,000
Soluble fraction	2837	358	2103	3267	2614	4813	4338	4647	4000	60,000
pH	8,09	8,98	8,48	8,65	8,83	8,76	8,77	8,71	–	> 6
Conductivity (μS/cm)	264	27,75	114,40	104,50	114,45	134,80	137,15	133,80	–	–

Table 7
Results of leaching tests of mixtures PMxSed50.

Parameters	Sediment	Sand	PM12Sed50	PM14Sed50	PM16Sed50	PM18Sed50	PM20Sed50	PM25Sed50	ISDI threshold	ISDND threshold
As	0,1	< 0,1	0,19	0,14	0,13	0,16	0,13	0,16	0,5	2
Ba	3	0,03	0,03	< 0,007	0,01	< 0,007	0,02	0,03	20	100
Cd	0,01	< 0,01	< 0,02	< 0,02	< 0,02	< 0,02	< 0,02	< 0,02	0,04	1
Co	–	<0,01	0,08	0,08	0,03	0,11	0,12	0,13	–	–
Cr	0,02	< 0,01	< 0,004	< 0,004	< 0,004	< 0,004	< 0,004	< 0,004	0,5	10
Cu	0,6	< 0,02	0,14	< 0,007	< 0,007	0,03	0,02	0,02	2	50
Mo	0,1	< 0,1	< 0,04	< 0,04	< 0,04	< 0,04	< 0,04	< 0,04	0,5	10
Ni	0,1	< 0,04	< 0,03	< 0,03	< 0,03	< 0,03	< 0,03	< 0,03	0,4	10
Pb	0,1	< 0,02	< 0,09	< 0,09	< 0,09	< 0,09	< 0,09	< 0,09	0,5	10
Sb	0,11	< 0,05	< 0,2	< 0,2	< 0,2	< 0,2	< 0,2	< 0,2	0,06	0,7
Se	0,07	< 0,11	< 0,1	< 0,1	0,07	0,08	0,09	0,13	0,1	0,5
Sn	–	< 0,06	< 0,09	< 0,09	< 0,09	< 0,09	< 0,09	< 0,09	–	–
V	–	0,03	0,13	0,11	0,08	0,09	0,09	0,1	–	–
Zn	1	< 0,03	0,03	< 0,01	< 0,01	< 0,01	< 0,01	< 0,01	4	50
Chlorides	36	< 10	17,5	13	10,5	11,50	12	23,5	800	15,000
Fluorides	20	< 5	11,5	10	6	6,5	5,7	4,9	10	150
Sulfates	270	< 10	165,5	141,5	163	175	180,5	191	1000	20,000
Soluble fraction	2837	358	3367	2857	3737	5656	2594	1362	4000	60,000
pH	8,09	8,98	8,63	8,65	8,51	8,58	8,62	8,67	–	> 6
Conductivity (μS/cm)	264	27,75	152,25	143,15	133,95	141,95	144,00	155,70	–	–

after the incorporation of the sediment in a polymer matrix, this value has decreased except for the PM12Sed50 mortar where the amount of binder is low, the fluoride value decreases when the quantity of resin increases.

The pH of the PMxSed50 mortar is almost stable and its value between the pH value of the sediment and the value of the sand. The soluble fraction increases with the increase of the mass fraction of the binder. The conductivity of the PMxSed50 mortar is small compared to the raw sediment but it is large compared to the sand. The PMxSed50 mortar of the different mass fraction of the binder is a non-inert and non-hazardous mortar. The explanation of the decrease in the chemical values of the raw sediment after the incorporation of the sediments in a polymer matrix, the sediment loads are covered by the binder which prevents the diffusion of the chemical elements in the solution. Mainly, the increase of the soluble fraction is bound to the resin.

3.11. SEM observation

Scanning electron microscopy (SEM) of hardened polymer mortar was performed and observations were made on the different formulations to investigate the sediment effect on the interface microstructure. The scanning electron microscope (SEM) analysis shows the good bonds between aggregates and epoxy resin. Hardened polymer mortar observation shows a good dense and consistent structure, which is in agreement of previous study [67,69]. Otherwise it can observe that the porosity in the composite is clearly influenced by the replacement of sand by sediment and the amount of epoxy resin/sediment in the matrices. This may also be due to the chemicals elements that make up the material in the sediments.

4. Conclusion and perspectives

This research paper has shown the feasibility of optimizing sediments in a polymer matrix with the packing density model l, this model can give approximate percentages of the constituents to obtain an optimal compactness of the mixture; the porosity of the mixture given by the model may be the approximate amount of binder to be added.

The curing time of the polymer mortar made by sediments is identical to that of the polymer mortar made by sand. Tests of flexural, compressive strength and modulus of elasticity have shown good results, mechanical properties are related to the amount of resin and the nature of sediments. From the determined mass fraction of the binder, the results of the mechanical tests of the polymer mortar made by sediment exceed the results of the mechanical tests of a polymer mortar made by standardized sand. The mechanical properties can be improved if the sediment is saturated with a solution that does not react with the resin or with a surface treatment of the sediment to increase the adhesion forces between the sediment and the matrix.

The polymer mortar made by sediment has good physical properties. Mercury porosity and water absorption are related to the amount of resin and the amount of sediment. There is a linear relationship between compressive strength and porosity for polymer mortar made with sediment unlike mortar made with sand. The water absorption of the polymer mortar made by sand is low compared to the polymer mortar made by sediment, this difference related to the high water content of the sediment.

The polymer mortar made by sediment showed good thermal properties when compared to the polymer mortar made by sand, the incorporation of the sediment in a polymer matrix has influenced the thermal properties. The polymer mortar made by sediment has shown good durability to chemical attack and thermal shock, the durability of the polymer mortar manufactured by sediment is related to the nature and quantity of the load and the amount of binder. The leaching test has shown that the epoxy resin has an important role of covering the load, this cover limits the diffusion of the chemical elements.

Acknowledgements

This project was initiated in the Hauts de France Region (France), collaboration IMT LILLE DOUAI and Neo Eco Recycling. The authors thank the European Regional Development Fund (ERDF) for their financial support to the project.

References

[1] Scordia P.-Y., Caractérisation et valorisation de sédiments fluviaux pollués et traités dans les matériaux routiers, 2008 203.
[2] E. Rozière, M. Samara, A. Loukili, D. Damidot, Valorisation of sediments in self-consolidating concrete: mix-design and microstructure, Constr. Build. Mater. 81 (2015) 1–10, https://doi.org/10.1016/j.conbuildmat.2015.01.080.
[3] M. Benzerzour, Y. Mamindy-Pajany, E. van Veen, M. Boutouil, N.E. Abriak, Beneficial reuse of Brest-Harbor (France)-dredged sediment as alternative material in road building: laboratory investigations, Environ. Technol. 39 (2018) 566–580, https://doi.org/10.1080/09593330.2017.1308440.
[4] F. Hamouche, R. Zentar, Effects of organic matter on physical properties of dredged marine sediments, Waste and Biomass Valorization. (2018) https://doi.org/10.1007/s12649-018-0387-6.
[5] N. Junakova, J. Junak, M. Balintova, Reservoir sediment as a secondary raw material in concrete production, Clean Techn. Environ. Policy 17 (2015) 1161–1169, https://doi.org/10.1007/s10098-015-0943-8.

[6] K. Siham, B. Fabrice, A.N. Edine, D. Patrick, Marine dredged sediments as new materials resource for road construction, Waste Manag. 28 (2008) 919–928, https://doi.org/10.1016/j.wasman.2007.03.027.

[7] V. Dubois, N.E. Abriak, R. Zentar, G. Ballivy, The use of marine sediments as a pavement base material, Waste Manag. 29 (2009) 774–782, https://doi.org/10.1016/j.wasman.2008.05.004.

[8] R. Zentar, D. Wang, N.E. Abriak, M. Benzerzour, W. Chen, Utilization of siliceous–aluminous fly ash and cement for solidification of marine sediments, Constr. Build. Mater. 35 (2012) 856–863, https://doi.org/10.1016/j.conbuildmat.2012.04.024.

[9] M. Amar, M. Benzerzour, A.E.M. Safhi, N.-E. Abriak, Durability of a cementitious matrix based on treated sediments, Case Studies Construction Mat. 8 (2018) 258–276, https://doi.org/10.1016/j.cscm.2018.01.007.

[10] J. Couvidat, M. Benzaazoua, V. Chatain, A. Bouamrane, H. Bouzahzah, Feasibility of the reuse of total and processed contaminated marine sediments as fine aggregates in cemented mortars, Constr. Build. Mater. 112 (2016) 892–902, https://doi.org/10.1016/j.conbuildmat.2016.02.186.

[11] A. el M. Safhi, M. Benzerzour, P. Rivard, N.-E. Abriak, I. Ennahal, Development of self-compacting mortars based on treated marine sediments, J. Building Eng. 22 (2019) 252–261, https://doi.org/10.1016/j.jobe.2018.12.024.

[12] C.-L. Hwang, L.A.-T. Bui, K.-L. Lin, C.-T. Lo, Manufacture and performance of lightweight aggregate from municipal solid waste incinerator fly ash and reservoir sediment for self-consolidating lightweight concrete, Cem. Concr. Compos. 34 (2012) 1159–1166, https://doi.org/10.1016/j.cemconcomp.2012.07.004.

[13] C.-W. Tang, H.-J. Chen, S.-Y. Wang, J. Spaulding, Production of synthetic lightweight aggregate using reservoir sediments for concrete and masonry, Cem. Concr. Compos. 33 (2011) 292–300, https://doi.org/10.1016/j.cemconcomp.2010.10.008.

[14] Benzerzour M., Maherzi. W., Amar M.A.A., Damidot D., J. Mater. Cycles Waste Manag. 20 (2018) 592, https://doi.org/10.1007/s10163-017-0626-0.

[15] A. el Mahdi Safhi, M. Benzerzour, P. Rivard, N.-E. Abriak, Feasibility of using marine sediments in SCC pastes as supplementary cementitious materials, Powder Technol. 344 (2019) 730–740, https://doi.org/10.1016/j.powtec.2018.12.060.

[16] A.L.G. Gastaldini, M.P. da Silva, F.B. Zamberlan, C.Z. Mostardeiro Neto, Total shrinkage, chloride penetration, and compressive strength of concretes that contain clear-colored rice husk ash, Constr. Build. Mater. 54 (2014) 369–377, https://doi.org/10.1016/j.conbuildmat.2013.12.044.

[17] A. Tironi, M.A. Trezza, A.N. Scian, E.F. Irassar, Assessment of pozzolanic activity of different calcined clays, Cem. Concr. Compos. 37 (2013) 319–327, https://doi.org/10.1016/j.cemconcomp.2013.01.002.

[18] M. Jamshidi, A.R. Pourkhorshidi, Modified polyester resins as an effective binder for polymer concretes, Mater. Struct. 45 (2012) 521–527, https://doi.org/10.1617/s11527-011-9779-9.

[19] J.I. Daniel, V.S. Gopalaratnam, M.A. Galinat, Reported by ACI Committee 544, (n.d.) 66.

[20] J.M. Reis, A.J. Ferreira, Assessment of fracture properties of epoxy polymer concrete reinforced with short carbon and glass fibers, Constr. Build. Mater. 18 (2004) 523–528, https://doi.org/10.1016/j.conbuildmat.2004.04.010.

[21] W. Lokuge, T. Aravinthan, Effect of fly ash on the behaviour of polymer concrete with different types of resin, Mater. Des. 51 (2013) 175–181, https://doi.org/10.1016/j.matdes.2013.03.078.

[22] J.P. Gorninski, D.C. Dal Molin, C.S. Kazmierczak, Comparative assessment of isophtalic and orthophtalic polyester polymer concrete: different costs, similar mechanical properties and durability, Constr. Build. Mater. 21 (2007) 546–555, https://doi.org/10.1016/j.conbuildmat.2005.09.003.

[23] K.S. Rebeiz, A.P. Craft, Polymer concrete using coal Fly ash, J. Energy Eng. 128 (2002) 62–73, https://doi.org/10.1061/(ASCE)0733-9402(2002)128:3(62).

[24] M.J. Hashemi, M. Jamshidi, Flexural Behavior of Polyester Polymer Concrete Subject to Different Chemicals, 28, 2015 7.

[25] E. Ghorbel, M. Haidar, Durability to chemical attack by acids of epoxy microconcretes by comparison to Cementitious ones, Adv. in Civil Eng. 2016 (2016) 1–15, https://doi.org/10.1155/2016/4728372.

[26] C. Vipulanandan, N. Dharmarajan, Flexural behavior of polyester polymer concrete, Cem. Concr. Res. 17 (1987) 219–230, https://doi.org/10.1016/0008-8846(87)90105-0.

[27] H. Abdel-Fattah, M.M. El-Hawary, Flexural behavior of polymer concrete, Constr. Build. Mater. 13 (1999) 253–262, https://doi.org/10.1016/S0950-0618(99)00030-6.

[28] M. Muthukumar, D. Mohan, Studies on polymer concretes based on optimized aggregate mix proportion, Eur. Polym. J. 40 (2004) 2167–2177, https://doi.org/10.1016/j.eurpolymj.2004.05.004.

[29] K.C. Radford, The mechanical properties of an epoxy resin with a second phase dispersion, J. Mater. Sci. 6 (1971) 1286–1291, https://doi.org/10.1007/bf00552042.

[30] Y. Nakamura, M. Yamaguchi, M. Okubo, T. Matsumoto, Effects of particle size on mechanical and impact properties of epoxy resin filled with spherical silica, J. Appl. Polym. Sci. 45 (1992) 1281–1289, https://doi.org/10.1002/app.1992.070450716.

[31] A.T. Dibenedetto, A.D. Wambach, The fracture toughness of epoxy-glass bead composites, Int. J. Polym. Mater. 1 (1972) 159–173, https://doi.org/10.1080/00914037208082114.

[32] J.M.L. Reis, Fracture and flexural characterization of natural fiber-reinforced polymer concrete, Constr. Build. Mater. 20 (2006) 673–678, https://doi.org/10.1016/j.conbuildmat.2005.02.008.

[33] H.G. Nguyen, S. Ortola, E. Ghorbel, Micromechanical modelling of the elastic behaviour of polymer mortars, Eur. J. Environ. Civ. Eng. 17 (2013) 65–83, https://doi.org/10.1080/19648189.2012.739787.

[34] M. Hassani Niaki, A. Fereidoon, M. Ghorbanzadeh Ahangari, a novel, Struct. Concr. 19 (2018) 366–373, https://doi.org/10.1002/suco.201700003.

[35] S.-C. Kou, C.-S. Poon, A novel polymer concrete made with recycled glass aggregates, fly ash and metakaolin, Constr. Build. Mater. 41 (2013) 146–151, https://doi.org/10.1016/j.conbuildmat.2012.11.083.

[36] Barbuta Marinela, Harja Maria, Baran Irina, Comparison of mechanical properties for polymer concrete with different types of filler, J. Mater. Civ. Eng. Vol 22 (7) (2019) (n.d.). https://ascelibrary.org/doi/abs/10.1061/(ASCE)MT.1943-5533.0000069 (accessed November 2, 2018).

[37] K.S. Rebeiz, S.P. Serhal, A.P. Craft, Properties of polymer concrete using Fly ash, J. Mater. Civ. Eng. 16 (2004) 15–19, https://doi.org/10.1061/(ASCE)0899-1561(2004)16:1(15).

[38] A. Kumar, G. Singh, N. Bala, Evaluation of flexural strength of epoxy polymer concrete with red mud and Fly ash, Int. J. Curr. Eng. Technol. 5 (2013).

[39] J.M.L. Reis, R. Chianelli-Junior, J.L. Cardoso, F.J.V. Marinho, Effect of recycled PET in the fracture mechanics of polymer mortar, Constr. Build. Mater. 25 (2011) 2799–2804, https://doi.org/10.1016/j.conbuildmat.2010.12.056.

[40] G. Sosoi, M. Barbuta, A.A. Serbanoiu, D. Babor, A. Burlacu, Wastes as aggregate substitution in polymer concrete, Procedia Manufacturing. 22 (2018) 347–351, https://doi.org/10.1016/j.promfg.2018.03.052.

[41] N. Benzannache, A. Bezazi, H. Bouchelaghem, M. Boumaaza, S. Amziane, F. Scarpa, Statistical analysis of 3-point bending properties of polymer concretes made from marble powder waste, sand grains, and polyester resin, Mech. Compos. Mater. 53 (2018) 781–790, https://doi.org/10.1007/s11029-018-9703-2.

[42] N.E. Marcovich, M.M. Reboredo, M.I. Aranguren, Mechanical properties of woodflour unsaturated polyester composites, J. Appl. Polym. Sci. 70 (1998) 2121–2131, https://doi.org/10.1002/(SICI)1097-4628(19981212)70:11<2121::AID-APP5>3.0.CO;2-Z.

[43] I. Ennahal, W. Maherzi, Y. Mamindy-Pajany, M. Benzerzour, N.-E. Abriak, Eco-friendly polymers mortar for floor covering based on dredged sediments of the north of France, J. Mat. Cycles Waste Manag. (2019) https://doi.org/10.1007/s10163-019-00843-3.

[44] A. Lecomte, J.-M. Mechling, C. Diliberto, Compaction index of cement paste of normal consistency, Constr. Build. Mater. 23 (2009) 3279–3286, https://doi.org/10.1016/j.conbuildmat.2009.05.005.

[45] Essai de compacité des fractions granulaires à la table à secousses: mode opératoire.. , Laboratoire central des ponts et chaussées, Paris, 2004.

[46] Elalaoui et al. , 2012, Mechanical and physical properties of epoxy polyme.pdf, (n.d.). https://ac.els-cdn.com/S0950061811003813/1-s2.0-S0950061811003813-main.pdf?_tid=033ade1e-482e-4ff2-b73d-a8c19960694f&acdnat=1535617709_40b87b5917863fa5655d02eab6da5bab (accessed August 30, 2018).

[47] P.J.R.O. Nóvoa, M.C.S. Ribeiro, A.J.M. Ferreira, Mechanical behaviour of Cork-modified polymer concrete, Mater. Sci. Forum 455–456 (2004) 805–809, https://doi.org/10.4028/www.scientific.net/MSF.455-456.805.

[48] Y. Ohama, K. Demura, Relation between curing conditions and compressive strength of polyester resin concrete, Int. J. Cem. Compos. Light. Concr. 4 (1982) 241–244, https://doi.org/10.1016/0262-5075(82)90028-8.

[49] M.E. Tawfik, S.B. Eskander, Polymer concrete from marble wastes and recycled poly (ethylene terephthalate), J. Elastomers & Plastics. 38 (2006) 65–79, https://doi.org/10.1177/0095244306055569.

[50] K.S. Rebeiz, Precast use of polymer concrete using unsaturated polyester resin based on recycled PET waste, Constr. Build. Mater. 10 (1996) 215–220, https://doi.org/10.1016/0950-0618(95)00088-7.

[51] D.M. Yemam, B.-J. Kim, J.-Y. Moon, C. Yi, Mechanical properties of epoxy resin mortar with sand washing waste as filler, Materials (Basel). 10 (2017) https://doi.org/10.3390/ma10030246.

[52] C. Vipulanandan, N. Dharmarajan, Flexural behavior of polyester polymer concrete, Cem. Concr. Res. 17 (1987) 219–230, https://doi.org/10.1016/0008-8846(87)90105-0.

[53] S.-Y. Fu, X.-Q. Feng, B. Lauke, Y.-W. Mai, Effects of particle size, particle/matrix interface adhesion and particle loading on mechanical properties of particulate–polymer composites, Compos. Part B 39 (2008) 933–961, https://doi.org/10.1016/j.compositesb.2008.01.002.

[54] M. Golestaneh, G. Amini, G.D. Najafpour, M.A. Beygi, Evaluation of mechanical strength of epoxy polymer concrete with si, 2010 6.

[55] P. Ravikumar, V. Ellappan, The mix proportion and strength of polyester resin concrete with various microfillers, (n.d.) 9.

[56] A.J.M. Ferreira, C. Tavares, C. Ribeiro, Flexural properties of polyester resin concretes, J. Polym. Eng. 20 (2000) https://doi.org/10.1515/POLYENG.2000.20.6.459.

[57] M.C.S. Ribeiro, P.R. Nóvoa, A.J.M. Ferreira, A.T. Marques, Flexural performance of polyester and epoxy polymer mortars under severe thermal conditions, Cem. Concr. Compos. 26 (2004) 803–809, https://doi.org/10.1016/S0958-9465(03)00162-8.

[58] M.C.S. Ribeiro, C.M.L. Tavares, M. Figueiredo, A.J.M. Ferreira, A.A. Fernandes, Bending characteristics of resin concretes, Mater. Res. 6 (2003) 247–254, https://doi.org/10.1590/s1516-14392003000200021.

[59] Y. Nakamura, M. Yamaguchi, M. Okubo, T. Matsumoto, Effect of particle size on mechanical properties of epoxy resin filled with angular-shaped silica, J. Appl. Polym. Sci. 44 (1992) 151–158, https://doi.org/10.1002/app.1992.070440116.

[60] X.L. Ji, J.K. Jing, W. Jiang, B.Z. Jiang, Tensile modulus of polymer nanocomposites, Polym. Eng. Sci. 42 (2002) 983–993, https://doi.org/10.1002/pen.11007.

[61] Mechanical properties of particulate composites, Composites, 4, 1973 93, https://doi.org/10.1016/0010-4361(73)90794-5.

[62] P.A. Webb, An Introduction To The Physical Characterization of Materials by Mercury Intrusion Porosimetry with Emphasis On Reduction And Presentation of Experimental Data, (n.d.) 23.

[63] M. Haidar, E. Ghorbel, H. Toutanji, Optimization of the formulation of micro-polymer concretes, Constr. Build. Mater. 25 (2011) 1632–1644, https://doi.org/10.1016/j.conbuildmat.2010.10.010.

[64] M.C.S. Ribeiro, J.M.L. Reis, A.J.M. Ferreira, A.T. Marques, Thermal expansion of epoxy and polyester polymer mortars—plain mortars and fibre-reinforced mortars, Polym. Test. 22 (2003) 849–857, https://doi.org/10.1016/S0142-9418(03)00021-7.
[65] C.P. Wong, R.S. Bollampally, Thermal conductivity, elastic modulus, and coefficient of thermal expansion of polymer composites filled with ceramic particles for electronic packaging, J. Appl. Polym. Sci. 74 (1999) 3396–3403, https://doi.org/10.1002/(SICI)1097-4628(19991227)74:14<3396::AID-APP13>3.0.CO;2-3.
[66] T.S. Chow, Effect of particle shape at finite concentration on thermal expansion of filled polymers, J. Polym. Sci. Polym. Phys. Ed. 16 (1978) 967–970, https://doi.org/10.1002/pol.1978.180160603.
[67] L. Agavriloaie, S. Oprea, M. Barbuta, F. Luca, Characterisation of polymer concrete with epoxy polyurethane acryl matrix, Constr. Build. Mater. 37 (2012) 190–196, https://doi.org/10.1016/j.conbuildmat.2012.07.037.
[68] M. Golestaneh, Evaluation of chemical resistance of polymer concrete in corrosive environments, Iranica J. Energy & Environ. 4 (2013) https://doi.org/10.5829/idosi.ijee.2013.04.03.19.
[69] Jiaqing Wang, et al., Mechanical and durability performance evaluation of crumb rubber-modified epoxy polymer concrete overlays, Constr. Build. Mater. 203 (2019) 469–480.